

1 Copyright WILEY-VCH Verlag GmbH & Co. KGaA, 69469 Weinheim, Germany, 2018.

2
3 Supporting Information

4
5
6 **Inspired by nature: facile design of nanoclay-organic hydrogel**
7 **bone sealant with multifunctional properties for robust bone**
8 **regeneration**

9
10 *Chung-Sung Lee, Hee Sook Hwang, Soyon Kim, Jiabing Fan, Tara Aghaloo and Min Lee**

11
12 Dr. C.S. Lee, Dr. H.S. Hwang, Dr. S. Kim, Dr. J. Fan, Prof. M. Lee

13 Division of Advanced Prosthodontics, University of California Los Angeles, CA 90095, USA

14
15 Prof. T. Aghaloo

16 Division of Diagnostic and Surgical Sciences, University of California Los Angeles, CA
17 90095, USA

18
19 Prof. M. Lee

20 Department of Bioengineering, University of California Los Angeles, CA 90095, USA

21
22 * Corresponding author:

23 **Min Lee, PhD,**

24 Professor

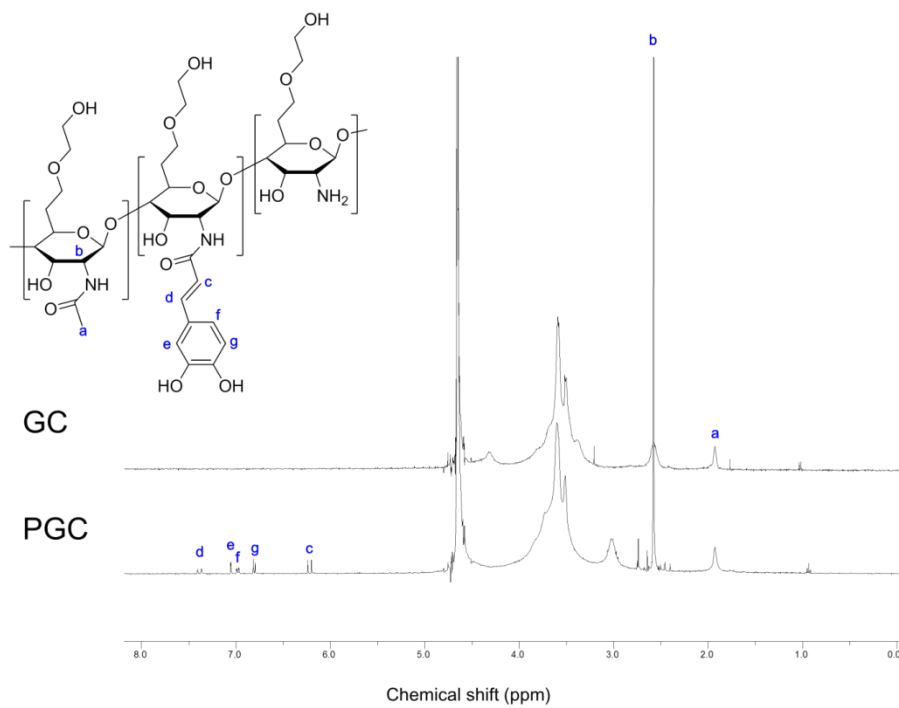
25 Division of Advanced Prosthodontics

26 Department of Bioengineering

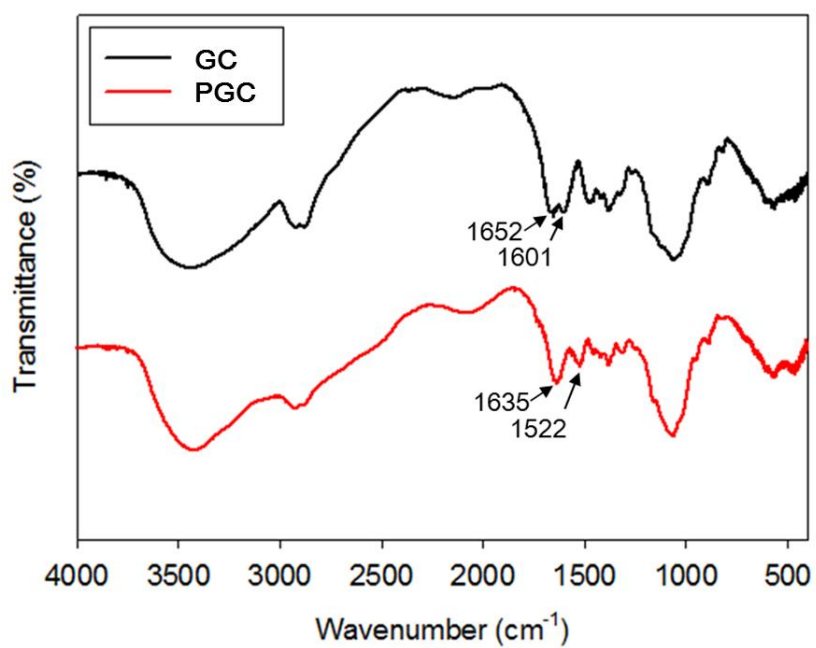
27 University of California, Los Angeles

28 Email: leemin@ucla.edu

29



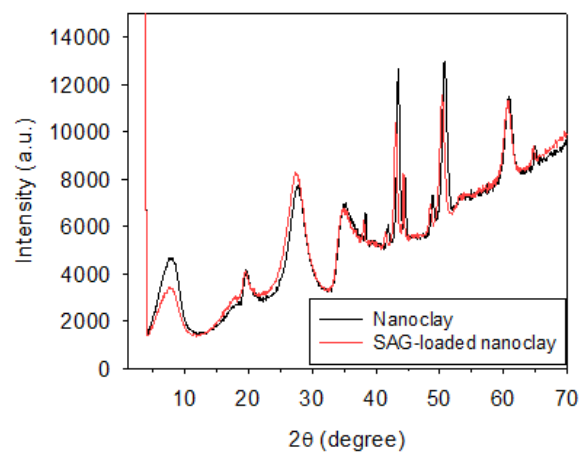
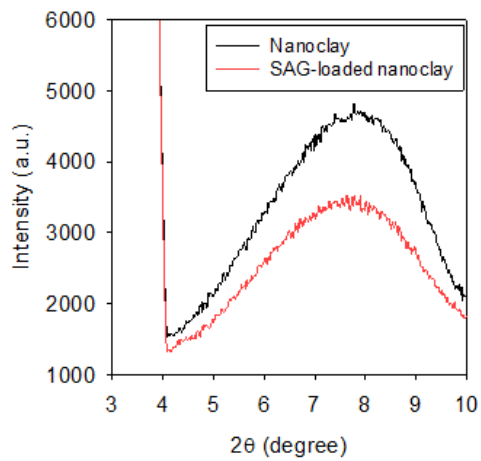
30
 31 **Figure S1.** ^1H NMR spectra of glycol chitosan (GC) and phytochemical conjugated GC (PGC)
 32 in D_2O .
 33



34

35 **Figure S2.** FT-IR spectra of GC and PGC.

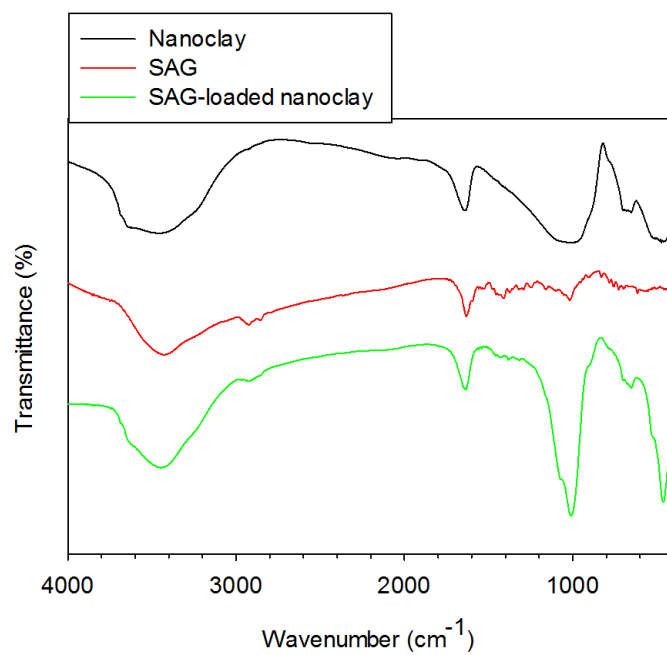
36



37

38 **Figure S3.** XRD patterns of nanoclay and SAG-loaded nanoclay.

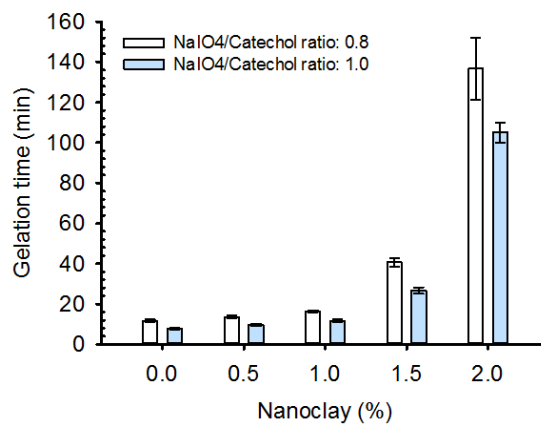
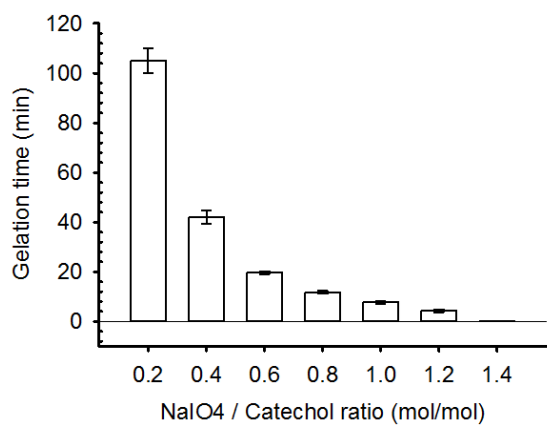
39



40

41 **Figure S4.** FT-IR spectra of nanoclay, SAG, and SAG-loaded nanoclay.

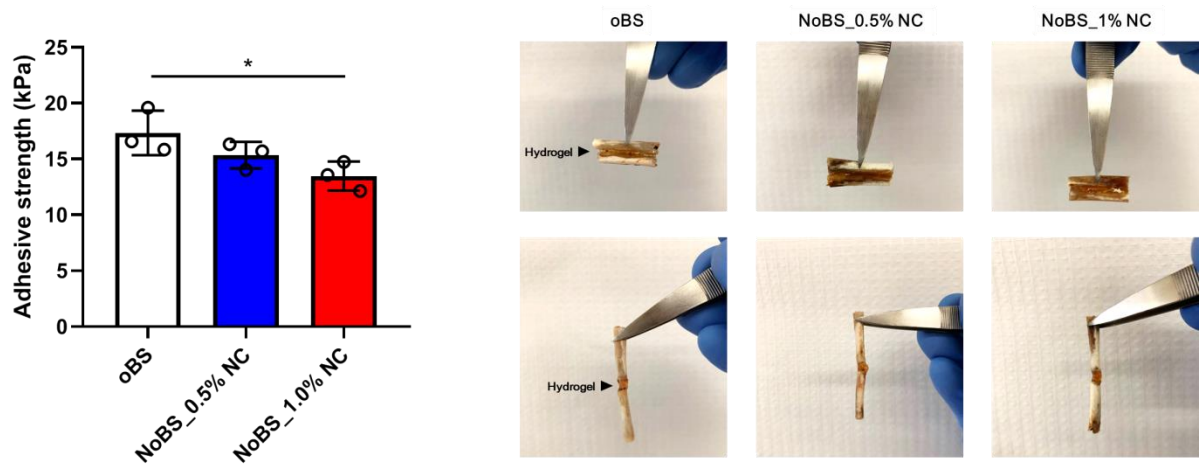
42



43

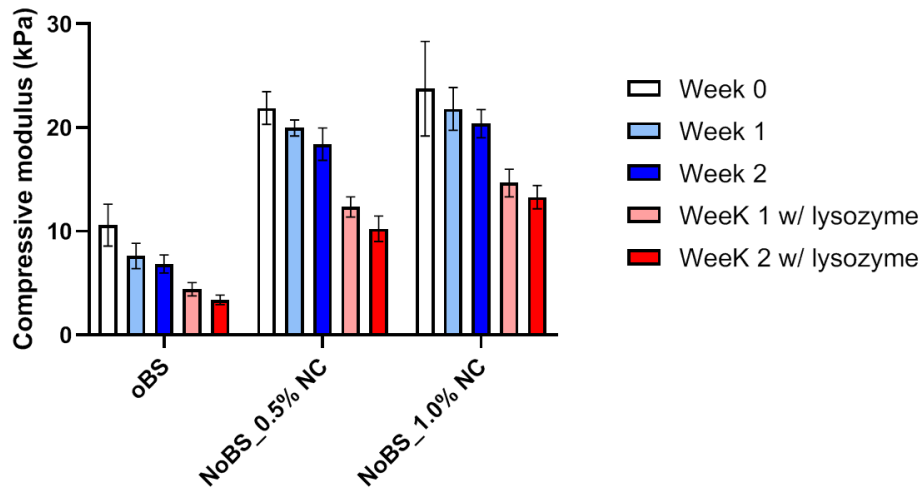
44 **Figure S5.** Gelation time of hydrogels at various NaIO₄/catechol group ratios and nanoclay
 45 contents.

46

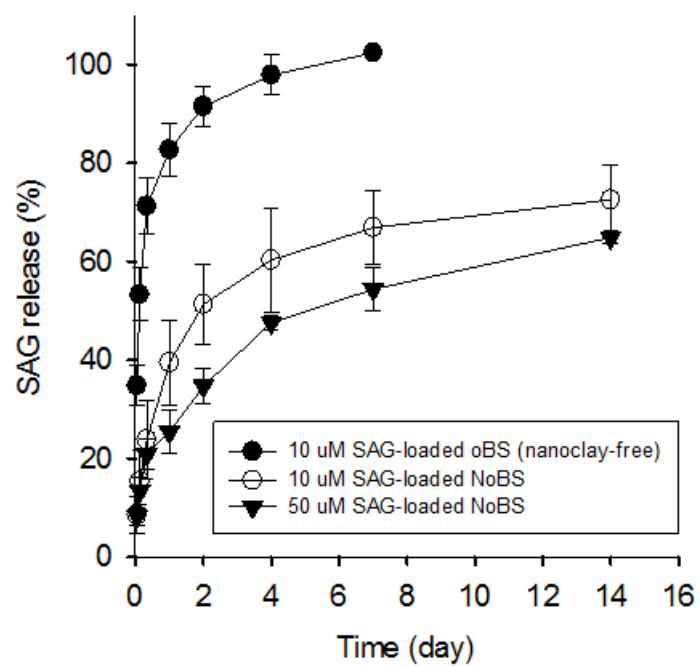


47

48 **Figure S6.** Adhesive strength of NoBS, and photography images of hydrogel adhesiveness to
 49 bone. Statistical analysis was determined by one-way ANOVA with Tukey's post hoc test; * P
 50 < 0.05 .



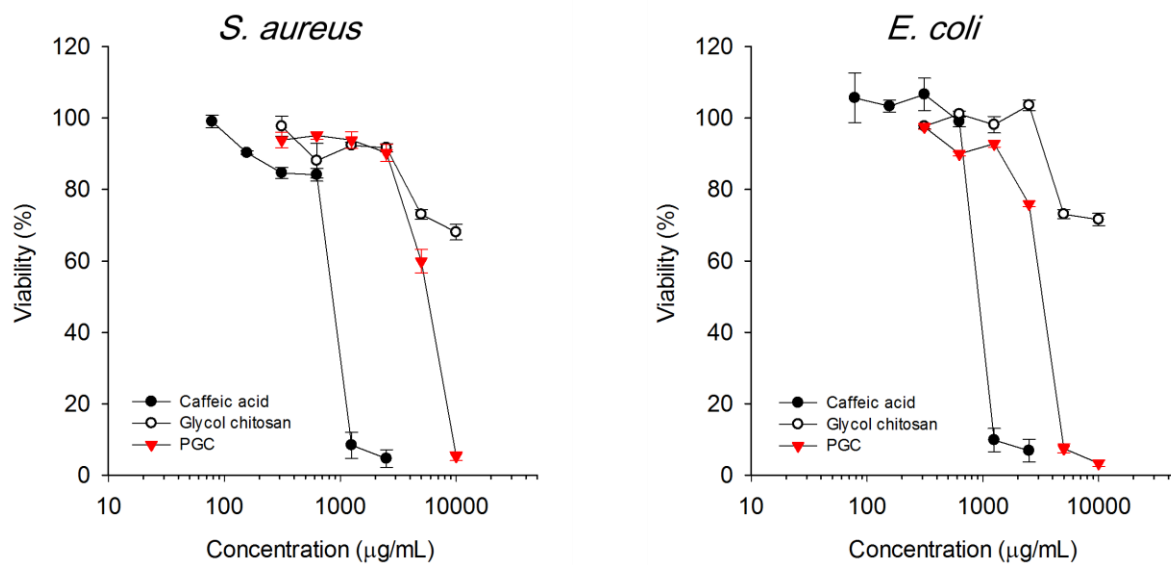
51
 52 **Figure S7.** The measurements of compressive modulus for NoBS after degradation for 2
 53 weeks. The hydrogels were incubated in the presence or absence of lysozyme (1 g L^{-1}) to
 54 facilitate degradation using lysozyme, a chitosan lytic enzyme.
 55



56

57 **Figure S8.** Time-lapsed release profiles of SAG from oBS and NoBSs.

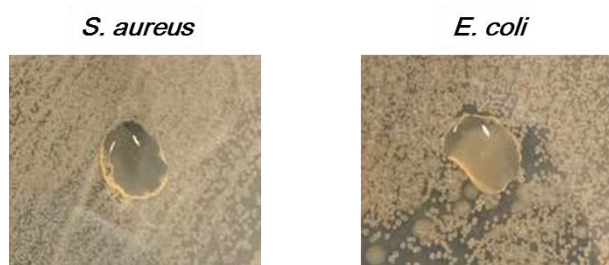
58



59

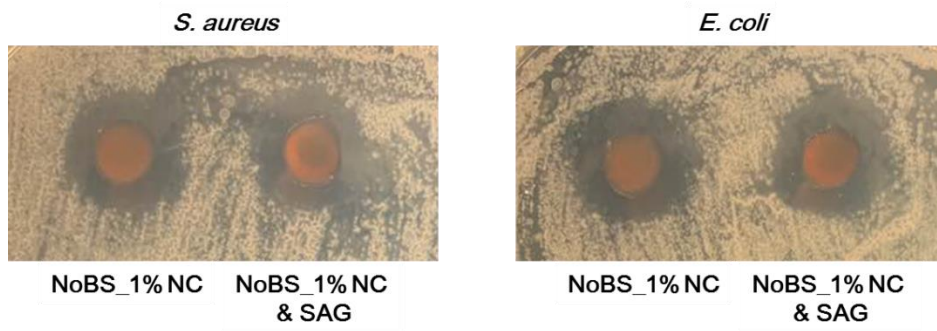
60 **Figure S9.** Viability test of caffeic acid, glycol chitosan and the PGC at various
 61 concentrations against *S. aureus* and *E. coli* for 24 h.

62



63
64
65
66

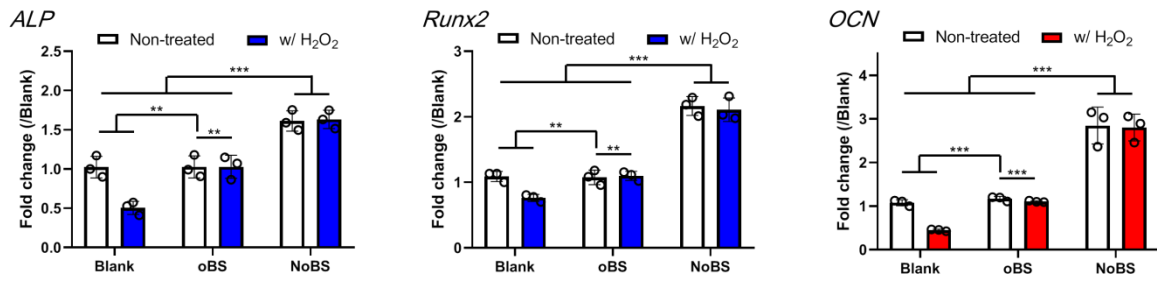
Figure S10. Representative image of bacterial colonies formed by **A)** *S. aureus* and **B)** *E. coli* with methacrylate chitosan hydrogel placed on the agar petri dish for a day.



67

68 **Figure S11.** Representative image of bacterial colonies formed by *S. aureus* and *E. coli* with

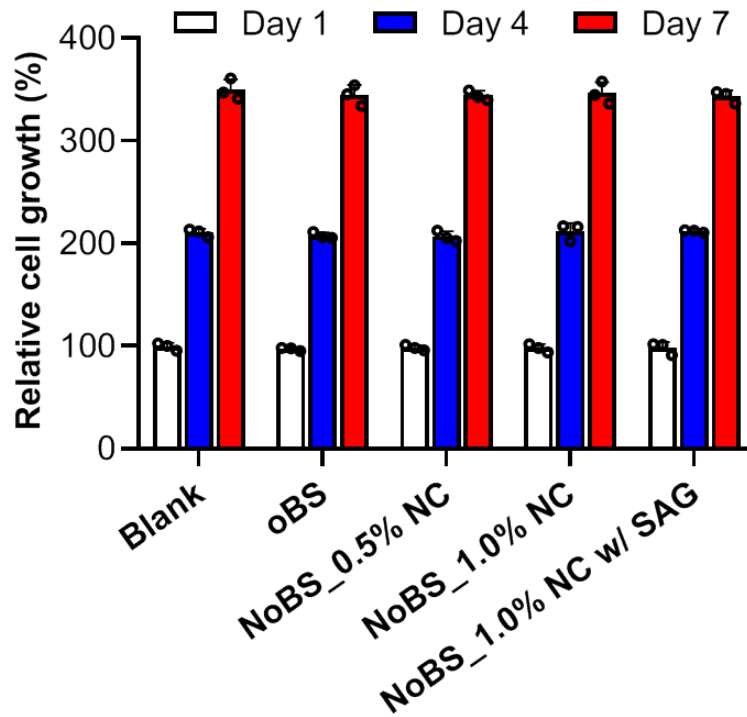
69 NoBS_1% NC in the presence or absence of SAG placed on the agar petri dish for a day.



70

71 **Figure S12.** Gene expression related to osteogenesis was evaluated with qRT-PCR with oBS
 72 and 1% nanoclay-NoBS in the presence or absence of 0.2 mM H₂O₂. *ALP* and *Runx2* were
 73 examined at day 4, and *OCN* was measured at day 14. Error bars indicate standard deviation
 74 (three independent cultures, n = 3), **p < 0.01, and ***p < 0.001 (ANOVA followed by
 75 Tukey's post hoc test).

76

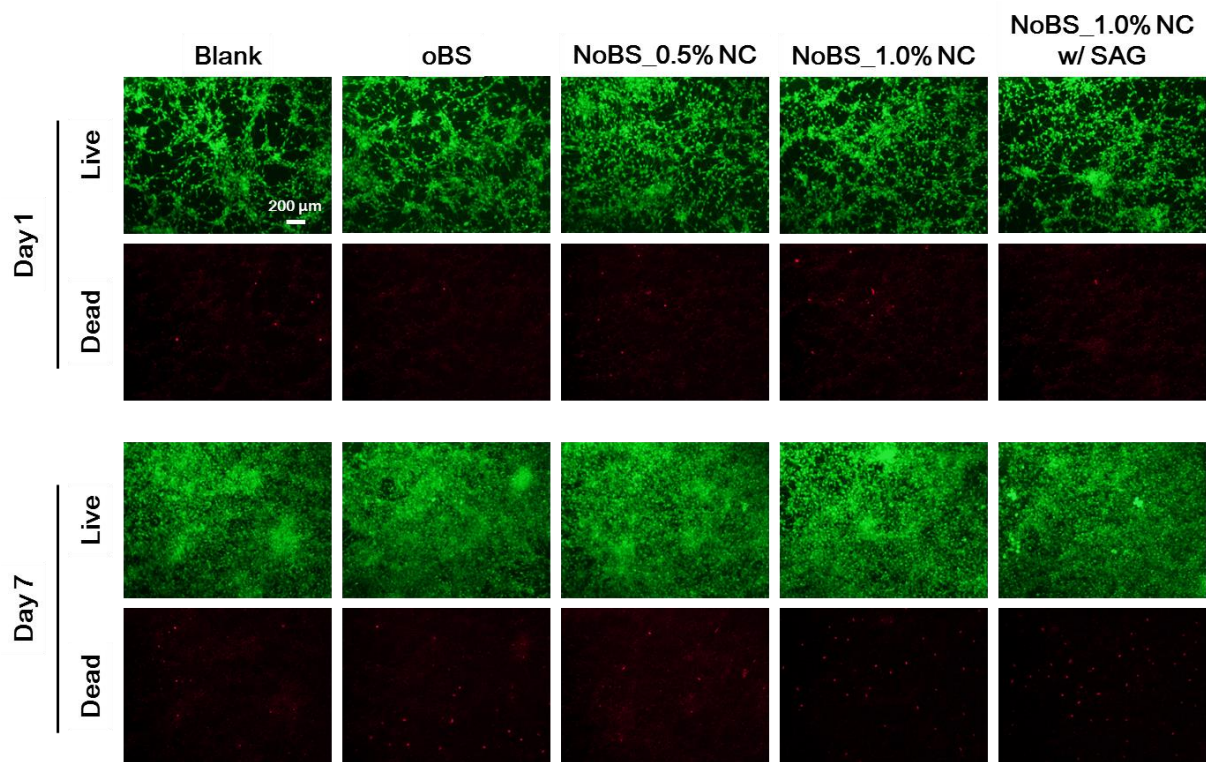


77

78 **Figure S13.** In vitro 2D cell proliferation assay of BMSCs incubated with oBS and NoBSs at
 79 various amounts of nanoclay (0.5 and 1.0%) in the presence or absence of 10 μ M SAG for 7
 80 days. The value was normalized by blank group of Day 1.

81

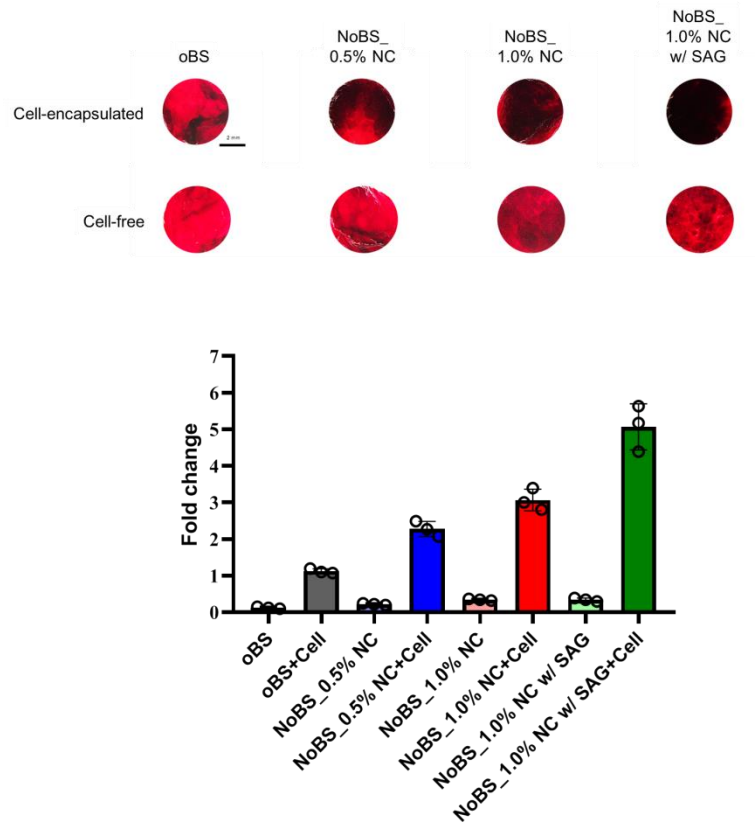
82



83

84 **Figure S14.** Representative confocal fluorescence images of BMSCs incubated with oBS and
 85 NoBSs at various amounts of nanoclay (0.5 and 1.0%) in the presence or absence of 10 μM
 86 SAG. The cells were stained with calcein AM (live cells, green fluorescence) and ethidium
 87 homodimer (dead cells, red fluorescence) at day 1 and day. Scale bar indicates 200 μm.

88



89
 90
 91
 92
 93

Figure S15. Alizarin red S staining of NoBS hydrogels. Relative colorimetric quantification of alizarin red S staining was compared between cell-encapsulating and cell-free groups. Scale bar indicates 2 mm. The concentration of SAG for SAG-containing groups was 10 μ M.

94 **Table S1.** Interplanar distances (d_{hkl}) and 2θ ($\lambda=1.54 \text{ \AA}$) of nanoclay and SAG-loaded
95 nanoclay determined by XRD data.

Diffraction plane (hkl)	Nanoclay		SAG-loaded nanoclay	
	θ ($^\circ$)	d (\AA) ¹⁾	θ ($^\circ$)	d (\AA)
(001)	7.83	11.29	7.65	11.56
(110, 020)	19.72	4.50	19.61	4.53
(004)	27.71	3.22	27.47	3.25
(130, 200)	35.05	2.56	34.73	2.58
(150, 240, 310)	50.78	1.80	50.36	1.81
(060, 330)	60.84	1.52	60.70	1.53

96 ¹⁾ The d -spacing was calculated by Bragg's equation.

97

98 **Table S2.** Elemental composition of the surface for oBS and NoBSs with various amounts of
 99 nanoclay (0.5 and 1.0%) in the presence or absence of 10 μ M SAG determined by energy
 100 dispersive X-ray spectrometry.

Atom %	oBS	NoBS_0.5% NC	NoBS_1.0% NC	NoBS_1.0% NC w/ SAG
C	54.57 \pm 1.41	48.59 \pm 1.59	47.79 \pm 1.48	47.19 \pm 1.79
N	13.30 \pm 4.99	-	-	-
O	32.13 \pm 1.59	37.23 \pm 1.15	38.33 \pm 1.04	38.24 \pm 1.25
F	-	1.59 \pm 0.51	1.77 \pm 0.52	1.99 \pm 0.60
Na	-	2.00 \pm 0.17	1.72 \pm 0.14	1.64 \pm 0.20
Mg	-	3.53 \pm 0.14	3.48 \pm 0.19	3.41 \pm 0.23
Si	-	5.89 \pm 0.18	5.66 \pm 0.22	5.57 \pm 0.26
S	-	-	-	0.66 \pm 0.11
Cl	-	1.18 \pm 0.13	1.25 \pm 0.11	1.30 \pm 0.13

101

102 **Table S3.** Sequences of primers for qPCR assay.

Primers	Forward	Reverse
GAPDH	AGGTCGGTGTGAACGGATTTG	TGTAGACCATGTAGTTGAGGTCA
ALP	GTTGCCAAGCTGGGAAGAACAC	CCCACCCCGCTATTCCAAAC
Runx2	CGGTCTCCTTCCAGGATGGT	GCTTCCGTCAGCGTCAACA
OCN	GGGAGACAACAGGGAGGAAAC	CAGGCTTCCTGCCAGTACCT
GSK-3	GCGTTCCCAAGAAGTGGCTTA	GGTCCAGCTTACGCATAATCTG
β -catenin	ATGGAGCCGGACAGAAAAGC	CTTGCCACTCAGGGAAGGA
PTCH	CAGGCTTCCTGCCAGTACCT	GACAATGATTCCAGCAGTCCAAG
Gli1	ACACATTACCAAGAAGCACCG	CAGCTGGTTTTCCCCTTTAAC

103